Effect of storage conditions on performance of nitrocellulose test strips used in lateral flow assays

Navjot Kaur[a], Mridul S. Kaimal[a], Bhushan J. Toley[ab]*
[a] Department of Chemical Engineering
Indian Institute of Science
Bangalore, India
560012

[b] Center for Biosystems Science and Engineering
Indian Institute of Science
Bangalore, India
560012

*Correspondence to:
Bhushan J. Toley
Department of Chemical Engineering
Indian Institute of Science
Bangalore, India, 560012
Phone: +91-80-22933114
Email: bhushan@iisc.ac.in

Abstract

The lateral flow assay (LFA) is the most commercially successful technology for conducting rapid diagnostic tests. However, the effect of long-term storage of membrane materials on the performance of the LFA has never been studied. In research laboratories, the turnover of raw materials used to fabricate LFAs could be quite low, leading to long storage times for membrane materials. We hypothesized that storage conditions and time for different constituent materials would have a notable effect on the performance of LFAs. We experimentally examined the impact of common lab storage conditions on the performance of different types of membrane materials typically used to fabricate LFAs, e.g. cellulose source pads, glass fiber conjugate pads, and nitrocellulose test membranes. Changes in flow properties, protein affinity, fluid imbibition/hydrophobicity, and LFA signal development were measured after storage under varied temperatures, humidity levels, and light and particulate matter exposure, for 1, 2 and 7 months. At the end of 7 months, the lateral imbibition rates decreased by 6±0.41x for nitrocellulose membranes exposed to light and dust, and 4.5±1.15x for nitrocellulose membranes stored at 37°C, in comparison to control membranes. These results were corroborated by measurements of free imbibition rates of sessile droplets placed on membrane surfaces. In contrast, cellulose wicking pads were found to be resilient to storage conditions and time, with a maximum reduction of 1.5x in lateral imbibition rates in comparison to control membranes. These results shed light upon the significant shift in performance parameters of diagnostic membranes with long term storage.

Introduction

Lateral flow assays (LFAs) are one of the best embodiments of point-of-care testing technologies. They are accessible, affordable, easy to use, rapid, and robust diagnostic tools that revolutionized the world of medical diagnosis in 1970s. Today, several commercially successful LFAs are available for testing for pregnancy, infectious agents, metabolic disorders, toxic metals in environment, dairy and food products(1,2). The ability to deliver quick and substantially reliable results at a reasonable price makes LFAs highly effective screening tools for disease diagnosis. Such diagnostic solutions help in reducing the economic burden on healthcare systems caused by testing every suspected patient using expensive confirmatory tests and aid in scaling up the preliminary screening of patients at a significant rate(3).

LFAs are made of porous membranes that exert capillary pressure on fluids. This results in powerless wicking of fluid through these membranes. The most commonly used format of an LFA consists of four sections (Fig. 1): sample pad (SP), conjugate pad (CP), test strip (TS) and wicking pad (WP). The test sample is added to the sample pad which is usually made of cellulose. The conjugate pad, made of glass fiber, stores dried labelled detection molecules that lead to signal generation in the LFA. The test strip is traditionally made out of nitrocellulose (NC) and consists of a test and a control line. The test line serves the function of capturing the analyte of interest while the control line helps in confirming flow of fluid through the test strip, acting as a measure of reliability of test results. The wicking pad acts as the major driver of fluid flow in an LFA after the test strip has been wetted by the test sample. It acts as a sink, absorbing the excess fluid that flows through the test strip. Unsaturated portions of the wicking pad continuously exert capillary pressure to ensure flow of (larger) sample volumes being tested in an LFA. Fig. 1 shows a schematic of a typical sandwich-type LFIA in which the test sample containing the analyte of interest is added to the sample pad. The sample flows through

the conjugate pad where labelled (gold nanoparticle, fluorophore, dyed polystyrene etc.) detection antibodies attach to the analyte of interest. This complex then flows past the test line where a capture antibody specific to the analyte of interest captures it, resulting in signal generation at the test line. The remaining antibodies that are not captured at the test line are captured at the control line.

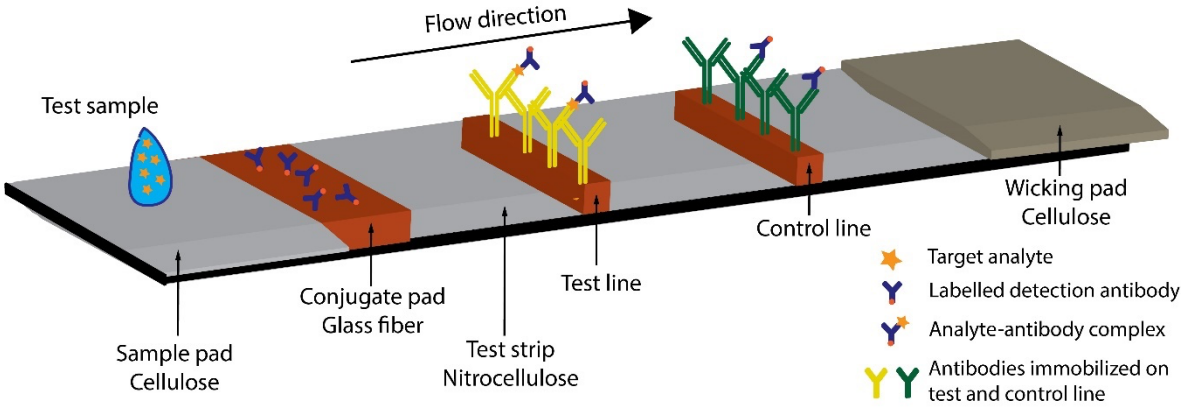

Figure 1. Schematic of the lateral flow immunoassay strip

Though these porous membranes lay the foundation of LFAs, not much is known about the effect of storage conditions on the characteristic properties of these membranes. The field of research on LFA development has been blooming over the years to improve the performance of LFA testing(4) by incorporating design changes(5–8), improving reaction kinetics and reaction chemistry(9–11), and improving detection labels(12–14). But the rate at which research groups utilize paper membranes, which form the backbone of LFAs, is very low and that leads to substantially long storage times for these membranes under varying lab conditions. Researchers continue to use these stored membranes for developing their LFA technologies, without much knowledge of the effect of storage conditions and time on the performance of these membranes. Because these membranes are stored in labs for at least a couple of months till up to several years over which they are used to develop LFAs, it becomes crucial to understand the effect of environmental factors on these membranes. Trumpie et. al(15)

highlighted the lack of understanding of membrane properties used for LFAs while reviewing the strengths and weaknesses of LFAs. Castro et al.(16) created a library of paper-specific properties pertaining to water saturation, evaporation flux, and effective permeability for common cellulose materials to inform design decisions for making more precise and reproducible paper-based microfluidic devices. This study created a well-curated database for researchers, but no comments were made on the age of membranes used and conditions they were stored in. Though LFA developers are aware of the importance of proper storage of membranes, a quantitative evaluation of the impact of different storage conditions and storage periods on membrane performance does not exist.

In this work, we experimentally quantify the effect of storage time and conditions on properties of porous membranes used in assembling LFAs, over a period of 7 months. To the best of our knowledge, this is the first investigation of this kind. Four different types of paper membranes corresponding to materials used for sample pad, conjugate pad, test strip, and wicking pad were stored under varying temperatures and humidity levels and exposed to light and dust. Conditions for storage were chosen such that they closely mimicked possible storage conditions existing in research labs over different parts of the world. Stored membranes were subsequently tested for their characteristics vital for efficient performance of LFAs. Initial pilot studies conducted for a storage period of one month revealed sample pad (CF1) and conjugate pad (Standard 17) materials to be quite robust with almost no loss in functionality when stored under different conditions. Hence, we continued our investigation for test strip and wicking pad materials. For NC test strip membranes (FF120), changes in protein affinity and fluid imbibition rates were recorded for storage over 7 months under the chosen storage conditions, whereas for cellulose wicking pads, changes in only fluid imbibition rate were recorded as its function in LFAs is to drive fluid flow. LFIAs were conducted using stored membranes at the

end of seven months to assess the overall impact of storage conditions on assay performance. This study highlights the requirement of due consideration that must be given to conditions of storage of test strip and wicking pad membranes.

Results and Discussion

Rationale for selection of storage conditions and performance parameters

Storage conditions evaluated in this study were chosen such that they resembled storage conditions present in research labs around the world. Three different temperatures (25°C/room temperature, 37°C, and 45°C) were tested to cover a wide range of geographical variations in temperature. RH levels were approximately 48.5%, 28.3%, and 15% for room temperature, 37°C and 45°C, respectively. Two other factors that could impact membrane performance are exposure to light and particulate matter, which were also studied. The performance parameters measured for different membrane types were chosen depending on the role of that membrane in an LFA. For example, signal generation on test and control lines in an LFA is strongly governed by i) the ability of NC to retain immobilized antibodies, and ii) the wicking rate of the membrane. The efficiency of retention of antibodies governs the efficiency of analyte capture and the wicking rate of the membrane governs the available reaction time at the test and control spots. NC test strips were, therefore, tested for changes in protein affinity and wicking rates on storage. Similarly, because the role of the wicking pad is to drive flow once the test membrane is wetted, changes in wicking rates were investigated for the wicking pad. The following terminology is used for the seven storage conditions that were investigated: (i) room temperature exposed to light_sealed (RTL-S), (ii) room temperature wrapped in aluminium foil to avoid exposure to light (dark)_sealed (RTD-S), (iii) room temperature, open to lab environment and light_unsealed (RTL-U), (iv) 45ºC_sealed (45-S) (v) 45ºC_unsealed (45-U), (vi) 37ºC_sealed (37-S) and (vii) 37ºC_unsealed (37-U). Wherever the storage

condition is suffixed by "_S (sealed)", parafilm was used to seal the lid with the bottom plate of the petri dish (Supplementary Information (SI); Fig. S1A (ii)). Else the petri dishes were kept open (SI Fig. S1B), exposed to the surrounding environment, and the storage condition is suffixed by "_U (unsealed)". Original packages of membranes, as ordered from manufacturers, were kept in a closed storage cabinet in the fabrication room and these membranes were used as controls for comparison with membranes stored under different challenge conditions. The control membranes are referred to as "stock membranes" hereafter.

Protein affinity of nitrocellulose membranes

To evaluate changes in protein affinity of NC membranes, different concentrations (1 µg/µL, 0.5 µg/µL and 0.25 µg/µL) of BSA were hand spotted on NC membranes after storage for 1 month, 2 months and 7 months. Protocol for protein staining was adopted from Metkar et al.(17) and optimized for our application. Protein spots were stained with Coomassie blue diluted in a staining solution comprising of methanol, acetic acid and water in 4:1:5 ratio. The same solution devoid of Coomassie blue was used for de-staining NC membranes to remove Coomassie blue non-specifically adsorbed on NC membrane. The intensity of blue color developed was analyzed to indicate the amount of protein retained by NC membranes. Fig. 2A shows representative images for protein staining experiments for NC membranes stored at 37°C for 1 month (37_S_1), 2 months (37_S_2) and 7 months (37_S_7). Scanned images of all membranes for different storage conditions and time are provided in SI Fig. S2, S3, and S4.

In order to better visualize performance of stored membranes in comparison with control stock membranes, protein spot intensities for membranes stored under different conditions were normalized by the mean spot intensity for corresponding concentrations spotted on stock membranes. Average normalized intensity for three protein concentrations (1 µg/µL, 0.5 µg/µL

and 0.25 µg/µL), tested in triplicates for each storage condition was plotted for 1 month (Fig. 2B), 2 months (Fig. 2C) and 7 months (Fig. 2D) of storage. Three protein concentrations were chosen to examine that any improvement or reduction in protein affinity was valid for a range of protein concentrations and not one single protein concentration. If spot intensity for stored membranes were equal to average intensity for control stock membranes, the normalized intensity would be 1 (dashed line; Fig. 2B-D). If protein affinity of the membrane had improved over time, the stained spots would be darker leading to normalized intensity greater than 1 while if protein affinity had reduced, then normalized intensity would be less than 1. The '*' symbol in Fig. 2B-D indicates statistically significant differences from stock membranes. A storage period of 1 month did not have any significant impact on protein affinity of membranes under any storage condition (Fig. 2B). After 2 months storage, protein affinity increased slightly for all storage conditions with most significant increase for membranes stored unsealed at 45°C (Fig. 2C; 45-U; $p<0.05$). After 7 months storage, a significant loss in protein retention was observed for exposure to light and dust (RTL-U; $p<0.05$); the remaining storage conditions performed similar to stock membranes. The highest p-value cut-off which was common for all three protein concentrations has been reported for each storage condition.

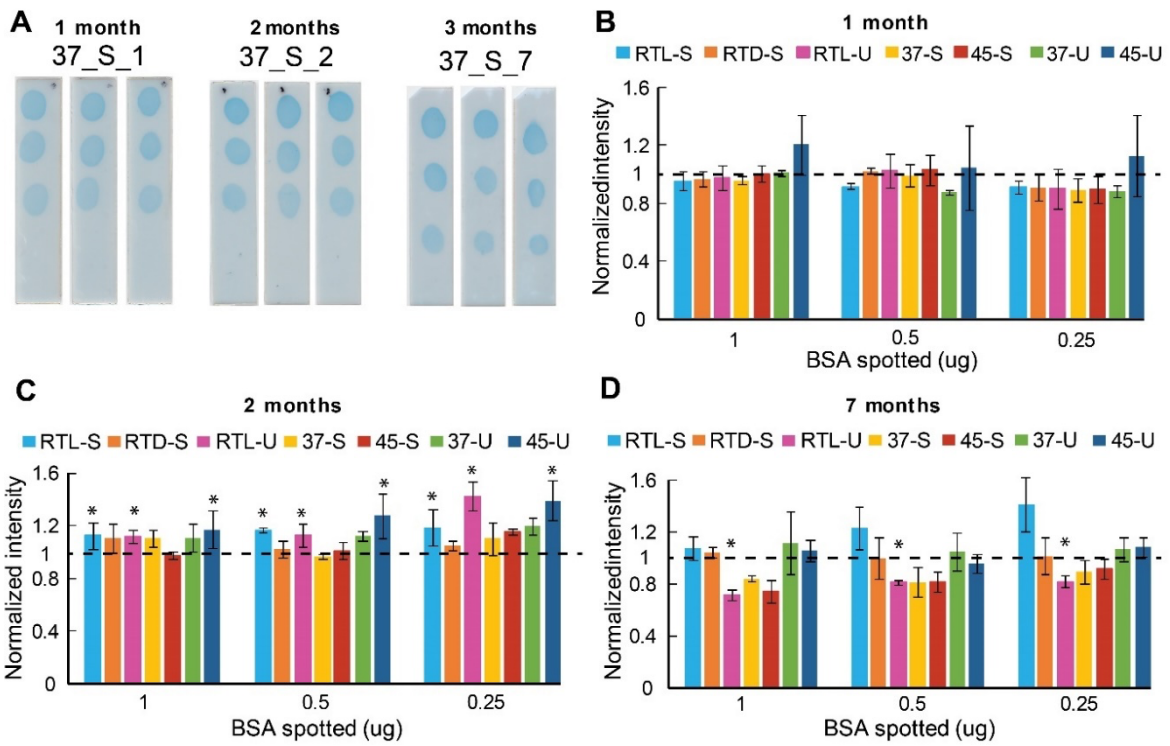

Figure 2. Protein affinity of nitrocellulose (NC) membranes over time. (A) Representative protein-staining results showing scanned images of membranes stored in sealed petri dishes at 37°C. 37_S_1, 37_S_2, and 37_S_7 represent membranes stored under condition 37-S for 1, 2, and 7 months, respectively. (B-D) Normalized intensity of stained protein spots on NC membranes for different storage conditions after storage for one (B), two (C), and seven (D) months. The color intensity for each spot was normalized by division with the mean color intensity for the corresponding concentration obtained from the stock membranes (N=3) tested on the same day. RTL-S: room temperature exposed to light-sealed, RTD-S: room temperature wrapped in foil-sealed, RTL-U: room temperature, open to lab environment and light-unsealed, 37-S: 37ºC-sealed, 45-S: 45ºC-sealed, 37-U: 37ºC-unsealed, and 45-U: 45ºC-unsealed.

Rate of lateral fluid imbibition

The lateral fluid imbibition rate for NC membranes was measured by incorporating NC membranes in a regular LFA format containing a sample pad, conjugate pad and a wicking pad (Fig. 3A), and the time required for fluid to wick 4 cm into the NC strip, t_{4cm}, was recorded. Membrane pieces stored under different conditions were tested for changes in wicking rates and t_{4cm} for stored membranes was normalized by division with the mean t_{4cm} (N=3) for stock membranes, which enabled measuring fold changes in lateral imbibition rates for different storage conditions. Lateral fluid imbibition rates for stock membranes were also compared over

time to keep a check on the changes developing in the stock membranes (SI Fig. S5). It was found that t_{4cm} values for stock membranes over the 7 months period were similar and, in the range, provided by the manufacturer.

After storage for 1 month (Fig. 3B), three storage conditions led to significant changes in lateral wicking rates – 37-U (4±0.3x change; $p<0.0001$; N=3), RTL-S (0.84±0.1x change, $p<0.05$; N=3) and RTL-U (1.41±0.05 x change; $p<0.001$; N=3). The remaining conditions (Fig. 3B; RTD-S, 37-S and 45-S) did not significantly alter wicking rates compared to stock membranes and hence normalized t_{4cm} values for these conditions were close to 1 (dotted line; Fig. 3B). Testing of wicking rates after 2 months of storage revealed increase in t_{4cm} for all conditions except for RTL-S and RTD-S (Fig. 3C). Following increments were observed in comparison with stock membranes – 45-U (1.8±0.2x change; $p<0.001$; N=3), 37-U (4±0.4x change; $p<0.0001$; N=3), RTL-U (3±0.5x change; $p<0.0001$; N=3), 37-S (1.48±0.1x change; $p<0.0001$; N=3) and 45-S (1.8±0.4x change; $p<0.0001$; N=3). Final evaluation of wicking rates after storage for 7 months demonstrated that except for RTD-S, all other conditions led to statistically significant increase in t_{4cm} – RTL-S (1.6±0.3x change; $p<0.05$; N=3), RTL-U (6±0.5x change; $p<0.0001$; N=3), 37-S (3±0.6x change; $p<0.01$; N=3), 45-S (2.5±0.03x change; $p<0.0001$; N=3), 37-U (4.6±1.15x change; $p<0.01$; N=3), and 45-U (1.84±0.07x change; $p<0.001$; N=3),. In general, it was observed that unsealed conditions (suffixed –U) led to significant changes in wicking rates for stored membranes. The condition denoted by RTD-S involved no exposure to light or dust and was stored at room temperature in the range of 23-25°C. We believe that membranes stored under this condition were exposed to conditions similar to stock membranes and hence wicking rates for both these conditions were in close agreement with wicking rates provided by the manufacturer.

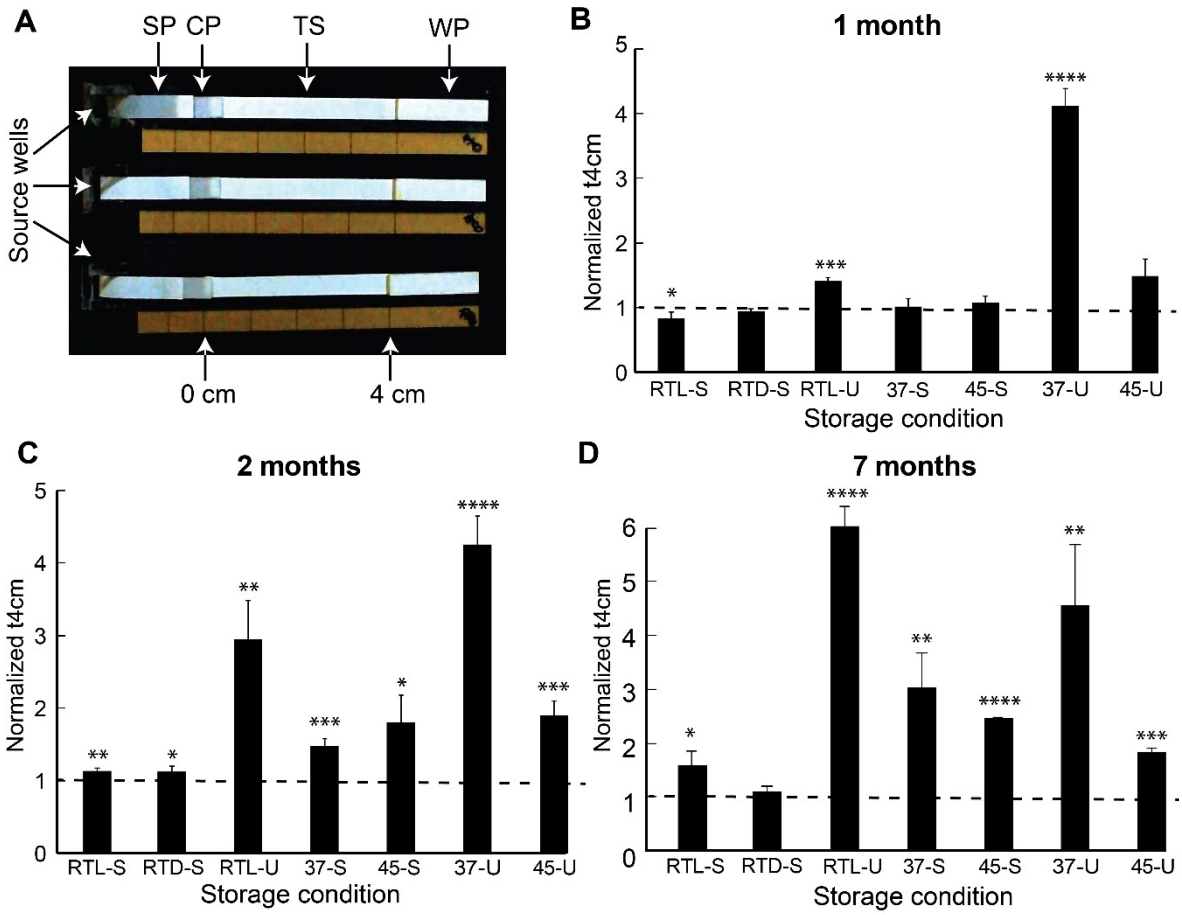

Figure 3. Lateral fluid imbibition rates for nitrocellulose (NC) membranes over time. (A) Image of the experimental set-up for measurement of fluid imbibition rate. (B-D) Normalized time, $t_{4cm,}$ required for fluid to wick 4 cm for NC membranes stored under different conditions after storage of 1 (B), 2 (C), and 7 (D)months. Wikcing times were normalized by the correspnding time for stock membranes. RTL-S: room temperature exposed to light-sealed, RTD-S: room temperature wrapped in foil-sealed, RTL-U: room temperature, open to lab environment and light-unsealed, 37-S: 37°C-sealed, 45-S: 45°C-sealed, 37-U: 37°C-unsealed, and 45-U: 45°C-unsealed.

Exposure to light (RTL-S) for a prolonged period of 7 months, even after maintaining temperature and humidity same as for (RTD-S) led to a slight slowing down of fluid flow (Fig. 3D). This can be explained by considering a possibility of changes in the chemical composition of proprietary chemicals deposited on NC membranes when exposed to light for a long period of time. Exposure to light and particulate matter in lab environment (RTL-U) led to consistent increase in t_{4cm} over time, reaching as high as 6±0.41 times of the stock after storage for 7 months (Fig. 3D). The physical appearance of membranes stored under this condition also

changed (SI Fig. S6, RTL-U) after storage for 7 months, while membranes stored under all other conditions appeared unchanged to the naked eye (SI Fig.S6). Slight browning of membrane surface and deposition of particulate matter was observed for RTL-U which could lead to blocking of pores in NC membranes and increase resistance to fluid flow. Exposure to elevated temperatures also increased t_{4cm} gradually over time. Elevated temperatures might also affect the proprietary chemical coating added to increase hydrophilic nature of NC membranes. It was also observed that after a period of 1 month, NC strips exposed to elevated temperatures started to curl (SI Fig. S7). Increased temperatures likely led to greater expansion of the plastic backing of NC membranes compared to the NC, resulting in inward curling of stored membrane pieces. Results for changes in lateral fluid imbibition rates for wicking pad are reported in SI S8 and S9.

Rate of free imbibition of sessile droplets

Changes in hydrophilicity of NC membranes were also investigated by measuring the free imbibition rates of sessile droplets placed on membrane surfaces for stock membranes and for those stored for 7 months. Figure 4A demonstrates imbibition of a 5 µL water droplet into NC membranes mounted on a goniometer platform. As the water droplet was absorbed by NC membranes, the size of the droplet and associated contact angles reduced (Fig. 4A; (ii)-(vi)). To compare imbibition rates across various storage conditions, a parameter, t_{15°, was defined as the time required for the contact angle to drop to 15 degrees. The parameter was normalized by the corresponding mean t_{15° (N=3) for stock membranes. t_{15° for storage conditions of RTL-S, RTD-S, RTL-U, 37-S, 45-S, 37-U, and 45-U were 4.5±1.5, 6±1.5, 13.1±0.9, 8.5±0.5, 4.3±0.4, 38±15.1 and 3.6±0.8 times, respectively, of t_{15° for stock membranes (Fig. 4B).

Fluid imbibition experiments highlighted an increase in hydrophobic nature of membranes stored under all the seven different storage conditions. For all storage conditions, the fold increase in normalized t_{15° was found to be greater than normalized t_{4cm}. This is likely because during lateral flow imbibition, only regions close to the fluid front are partially saturated(18) and provide capillary pressure for wicking; regions close to the infinite volume fluid source are close to 100% saturation and only act as conduits for flow. On the other hand, for free imbibition of sessile droplet, most of the wetted membrane volume would remain partially saturated and continue to provide capillary pressure for fluid flow. Because flow in the free imbibition of sessile drop case is governed by capillary pressures over a larger area than that in lateral flow, there was likely a larger effect of storage on sessile drop imbibition rates than lateral imbibition rates.

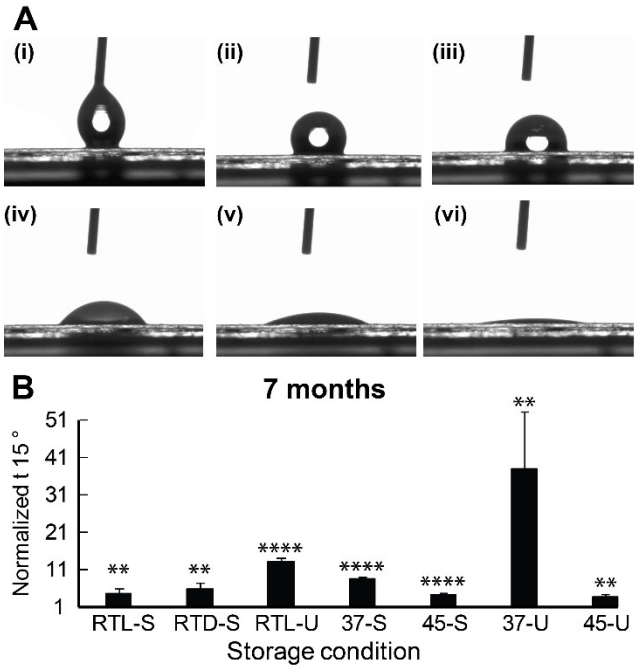

Figure 4. Rate of free imbibition of sessile droplets in nitrocellulose (NC) membranes after storage for 7 months. (A) Side view timelapse images of a water droplet imbibing into a NC membrane. (B) Time required for contact angles to drop to 15° (t_{15°) for different storage conditions. RTL-S: room temperature exposed to light-sealed, RTD-S: room temperature wrapped in foil-sealed, RTL-U: room temperature, open to lab environment and light-unsealed, 37-S: 37°C-sealed, 45-S: 45°C-sealed, 37-U: 37°C-unsealed, and 45-U: 45°C-unsealed.

pfHRP2 lateral flow assay testing using stored membranes

In previous experiments, protein retention capability and imbibition rates were evaluated as indirect measures of LFA performance. Next, lateral flow assay signals from stored membranes were directly measured. A pfHRP2 lateral flow immunoassay was conducted in NC membranes stored for a period of 7 months. LFAs were conducted in vertical format to ensure fluid flow purely by wicking. Sample pads and conjugate pads were eliminated to avoid introduction of additional variations in assay performance due to their presence. Endpoint LFA results were captured using a scanner (Fig. 5A; (i)-(viii)). Scanned images of replicates for membranes stored under all storage conditions are reported in SI Fig. S10. None of the storage conditions were observed to have a deleterious effect on LFA performance. Test spots detectable by naked eye appeared for all storage conditions while intensity of control spots varied for different conditions.

The test spot intensity for each stored membrane (N=3 per storage condition) was normalized by division with the mean test spot intensity (N=3) for stock membranes. LFA signals for all storage conditions (Fig. 5B, RTL-S. RTD-S, RTL-U, 37-S, 45-S, and 45-U) except one (Fig. 5B, 37-U) demonstrated unexpected statistically significant improvements in comparison to stock membranes (Fig. 5B). Normalized spot intensities were found to be greater than 1 with improvement of 21.7%, 16.1%, 30.5%, 18.6%, 16.6%, and 9.2% in signal intensity for storage conditions denoted by RTL-S, RTD-S, RTL-U, 37-S, 45-S, and 45-U, respectively. Reduction by 4.2% in signal intensity was observed for 37-U storage condition but the reduction was not found to be statistically significant. LFA results for 37-U condition were the only anomaly observed in this storage study. As protein retention was not substantially affected by storage conditions and time, we believe that improvement in LFA signal intensities was due to significant decrease in the fluid imbibition rates for NC membranes. Results for flow

experiments revealed that t_{4cm} for RTL-U, 37-S, 45-S, 37-U, and 45-U storage conditions at least doubled after storage for 7 months (Fig. 3D) and increased to almost 6±0.41 times for RTL-U. While t_{4cm} for RTL-S and RTD-S storage conditions were not extremely affected, normalized fluid imbibition rate for all conditions at the end of 7 months was greater than 1 (Fig. 4B). Increase in t_{4cm} would have led to slowing of fluid flow in test strip, providing more time for reaction components to react at test and control spots. Greater reaction times would allow a higher number of analyte molecules to be captured at the test spot, resulting in darker signal intensities. Note that long-term storage is not being proposed as a method to enhance signal intensities in LFAs. Our purpose is to highlight the drift in the performance of LFAs caused by long term storage of materials.

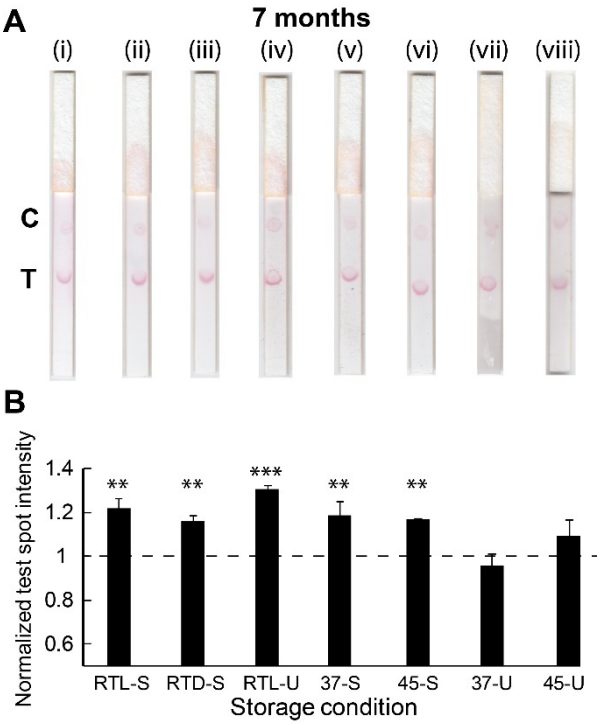

Figure 5. Performance of lateral flow immunoassays (LFIAs) in stored membranes (7 months) (A) End-point images of LFIAs conducted in stored NC membranes (i) Control stock membranes, (ii) RTL-S: room temperature exposed to light-sealed, (iii) RTD-S: room temperature wrapped in foil-sealed, (iv) RTL-U: room temperature, open to lab environment and light-unsealed, (v) 37-S: 37°C-sealed, (vi) 45-S: 45°C-sealed, (vii) 37-

U: 37°C-unsealed, and (viii) 45-U: 45°C-unsealed. B. Normalized intensity of LFA test spots for membranes stored under different conditions. RTL-S: room temperature exposed to light-sealed, RTD-S: room temperature wrapped in foil-sealed, RTL-U: room temperature, open to lab environment and light-unsealed, 37-S: 37°C-sealed, 45-S: 45°C-sealed, 37-U: 37°C-unsealed, and 45-U: 45°C-unsealed.

Conclusion

In this study, the effect of common lab storage conditions and storage periods on the performance of diagnostic paper membranes was evaluated by quantifying protein affinity, wicking rates, and membrane hydrophobicity. Prolonged storage of membranes under challenge conditions led to a significant reduction in fluid imbibition rates. For the specific application of LFIAs tested here, prolonged storage led to an unexpected marginal improvement in signal intensities. However, for other microfluidic paper-analytical devices, such changes could severely impact device performance. For example, sequential delivery in 2-dimensional paper networks (2DPNs) would be hampered by even slight changes in wicking rates. This study, thus, highlights the importance of proper membrane storage for reproducible performance of paper-based analytical devices.

Materials and Methods

Storage conditions

Rectangular pieces of NC (30 mm X 6 mm and 42.5 mm X 4 mm, FF120, GE healthcare) and CFSP (65 mm X 4 mm, 20300, Millipore) were cut using a 50 W CO_2 laser in a VLS 3.60 laser engraver (Universal Laser Systems, Scottsdale, AZ) and stored in a 100 mm petri dish. SI Fig. S1 shows representative images to familiarize readers with the way paper membranes were stored under different conditions. For room temperature conditions, petri dishes were kept on

a shelf in the fabrication lab (Fig. S1A), which housed equipment like a CO2 laser cutter, 3D-printer, a desktop computer, a laptop, a flatbed scanner, and two custom made flow imaging set-ups. Fabrication materials like all types of paper membranes, acrylic sheets, PDMS tape were stored in this lab, and it was frequently visited by many members of the lab on a daily basis. A temperature and relative humidity meter were used to keep a record of temperature and RH in the fabrication room and incubators over the storage period.

Protein affinity measurements of nitrocellulose membranes

NC membranes (30 mm X 6 mm) were tested for protein affinity by Coomassie blue staining of different concentrations of bovine serum albumin (BSA, A2153, Sigma) spotted on NC membranes. Protein staining was performed using 0.0025% of Coomassie blue diluted in a staining solution comprising of methanol, acetic acid and water in 4:1:5 ratio. The same solution devoid of Coomassie blue was used for de-staining NC membranes. Membranes stored under different storage conditions were taken out on the day of testing, and three spots of 1 µL each of 1, 0.5 and 0.25 µg/µL BSA were spotted on the NC strips. 1 µL of water was also spotted as a control for background intensity subtraction. Three stored membrane pieces were tested for each storage condition. BSA-spotted strips were dried in an incubator at 37^{o}C for 30 minutes. Strips were then placed in 2 mL centrifuge tubes containing 1.7 mL of Coomassie blue staining solution, enough to submerge entire strip lengths. After 20 minutes of staining, strips were transferred to 2 mL tubes containing 1.7 mL of de-staining solution and were left submerged in de-staining solution for 20 minutes. End-point protein stain intensities were scanned using a flatbed scanner (Canon LiDe 220). Image analysis was performed in ImageJ by creating a circular region of a fixed diameter to mark the stained protein spots and calculating mean pixel intensity in the red channel. Background subtracted spot intensity, $I_{backsub}$ was calculated as(19):

$$I_{backsub} = \frac{(I_{spot} - I_{Bg})}{(0 - I_{Bg})}$$

where:

I_{spot}: Intensity of stained protein spot

I_{Bg}: Intensity of strip where water was spotted to quantify background intensity

Student's t-tests (one-tail, equal variances) were used to compare the stained protein spot intensities for different storage conditions against stock membranes for each concentration of BSA spotted on NC. $I_{backsub}$ of triplicates for each concentration and storage condition was compared with triplicates for each concentration on stock membranes to obtain respective p-values.

Lateral flow imbibition rate measurements

Laser cut pieces of NC membranes (42.5 mm X 4 mm) stored under different storage conditions were used to assemble LFA strips on the day of the experiment. For fabricating control strips, sample pad (20 mm X 4 mm, CF1, GE Healthcare life Sciences), conjugate pad (10 mm X 4 mm, Standard 17, GE Healthcare Life Sciences (Bangalore, India),) and wicking pad (20 mm X 4 mm, CFSP, (new code C083), Sigma-Aldrich) were laser cut each time from their respective stocks stored in the membrane storage cabinet kept in fabrication room. LFA strips were fabricated using pressure sensitive adhesive (PSA; 3M^{TM} 9731) as the backing material. Fiducial marks were made at intervals of 1 cm on an extension of the PSA backing, which aided in measuring the distance travelled by the fluid front.

The experimental set-up for measuring the rate of lateral imbibition was designed to test triplicates for each storage condition at a time. The platform included three wells and LFA strips were arranged such that sample pads were slightly bent to dip into source wells, ensuring that fluid flowed purely by wicking. Flow experiments were conducted inside a humidity

chamber with RH maintained between 85 to 90% by lining the chamber with wet tissues. The base of the platform was made of black acrylic to reduce background noise while imaging. Forty µL water was added slowly to the wells by a syringe needle piercing through a silicone window designed for fluid addition. Flow of water through LFA strips was recorded from the top using a Logitech webcam (C525, Logitech Newark, CA) mounted on an adjustable stand. Time-lapse imaging was performed using HandyAvi (AZcendant, Tempe, AZ) at the rate of 4 frames per second (fps). The time required by the fluid front to reach the 4 cm marking (t_{4cm}) was obtained by analyzing video frames in ImageJ. Flow experiments were conducted in a similar fashion for CFSP wicking pads (65 mm X 4 mm) with 160 µL of water, the only difference being that instead of fabricating the whole LFA assembly, only CFSP was directly tested for wicking rates (t_{4cm}) to avoid excessive use of other valuable paper membranes.

Rate of free imbibition of sessile droplets

Fluid imbibition study for NC membranes (20 mm X 3 mm) were performed using a goniometer (OCA 25, Dataphysics Instruments, Germany) that measured contact angles for a drop of fluid added on to a surface. The setup consisted of an automatic fluid dispenser, an adjustable platform for fixing the membrane, and a telescopic camera connected to a computer to visualize the contact angles. NC strips were attached to the horizontal platform using a backing card (KN-PS1060.18, Kenosha). A 5 µL water droplet was dispensed selecting the slow dispense rate option and the droplet was allowed to be completely wicked by the membrane. Imbibition of the water droplet into the membrane was recorded at 20fps. The instrument software (SCA 20 module) automatically calculated the contact angle for different time points and results were plotted as variation of contact angle against time.

pfHRP2 lateral flow assay in stored membranes

Stored NC membranes (32 mm X 3 mm) were hand spotted using a stencil as a guide to produce consistent spots for LFA testing. Anti-pfHRP2 (1 µL of 1 mg/mL, # MPFM-55A, ICLLabs, Oregon) antibody was hand spotted at the test spot and 1 µL of goat anti-mouse antibody (1 mg/mL, GeNei labs, Bangalore) was hand spotted at the control spot. Sample pads and conjugate pads were not used in this set of experiments to avoid excessive use of porous membranes and to only measure performance changes in NC membranes. LFA testing was performed in a vertical format. An NC membrane attached to a wicking pad at one end using PSA as backing was directly dipped into a well of a 96-well ELISA plate. The sample solution consisted of 30 µL of pfHRP2 (500ng/mL, # AG55-0092-Z ICLLabs, Oregon), 1% BSA (A2153, Sigma), and 0.05% Tween-20 (Genei Laboratories Pvt. Ltd.) mixed with 10 µL of gold nanoparticle (AuNP, 40 nm, 20OD) conjugated to anti-pfHRP2 antibody (Gold Conjugation Kit, ab154873, Abcam). Membranes stored under different conditions were tested for pfHRP2 LFA performance after 7 months of storage. The assay run time was fixed at 30 minutes, following which, NC membranes were scanned using a flatbed scanner and images were analyzed using the green channel in ImageJ.

Acknowledgments:

This work was supported by an extramural research grant from the Science and Engineering Research Board, India (EMR/2016/006029), an Innovative Young Biotechnologist award from the Department of Biotechnology, India (BT/010/IYBA/2016/07), a Grand Challenges Exploration award from the Bill & Melinda Gates Foundation (OPP1182249), a Grand Challenges Exploration-India award from BIRAC-India, and by the Saroj Poddar Foundation in the form of a Young Investigator award, all to B.J.T; and by the Ministry of Human Resource Development (MHRD), India, in the form of graduate student support to N.K. We acknowledge

Prof. Susmita Dash, Mr Akshay Sharma and Ms Pranjal Agrawal for assisting us with measurement of free imbibition of sessile droplets using the goniometer available in Prof. Susmita Dash's lab.

Supporting Information: S1. Representative images depicting storage of membranes under different conditions; S2. Scanned images for protein staining experiments after storage period of 1 month; S3. Scanned images for protein staining experiments after storage period of 2 months; S4. Scanned images for protein staining experiments after storage period of 7 months; S5. Wicking rate for stock membranes over time; S6. Physical appearance of NC membranes after seven months of storage under different conditions; S7. Curling up of NC membranes on storage at high temperatures; S8. Rate of lateral fluid imbibition for wicking pad membranes; S9. Physical appearance of cellulose membranes after seven months of storage under different conditions; S10. Scanned images for LFIAs conducted in stored NC membranes.

References:

1. Ngom B, Guo Y, Wang X, Bi D. Development and application of lateral flow test strip technology for detection of infectious agents and chemical contaminants: A review. Anal Bioanal Chem. 2010;397(3):1113–35.
2. Sajid M, Kawde AN, Daud M. Designs, formats and applications of lateral flow assay: A literature review. J Saudi Chem Soc. 2015;19(6):689–705.
3. Koczula KM, Gallotta A. Lateral flow assays. Essays Biochem. 2016;60(1):111–20.
4. Bishop JD, Hsieh H V., Gasperino DJ, Weigl BH. Sensitivity enhancement in lateral flow assays: A systems perspective. Lab Chip. 2019;19(15):2486–99.
5. Jenkins JA, Dube L, Luo Y, Chen J, Fan TH, Lei Y, et al. A polymer hydrogel modified lateral flow sensing platform. Sensors Actuators, B Chem [Internet].

2018;262:493–8. Available from: https://doi.org/10.1016/j.snb.2018.01.214

6. Shen M, Li N, Lu Y, Cheng J, Xu Y. An enhanced centrifugation-assisted lateral flow immunoassay for the point-of-care detection of protein biomarkers. Lab Chip. 2020;20(15):2626–34.

7. Rey EG, O'Dell D, Mehta S, Erickson D. Mitigating the Hook Effect in Lateral Flow Sandwich Immunoassays Using Real-Time Reaction Kinetics. Anal Chem. 2017;89(9):5095–100.

8. Rey E, Jain A, Abdullah S, Choudhury T, Erickson D. Personalized stress monitoring: a smartphone-enabled system for quantification of salivary cortisol. Pers Ubiquitous Comput. 2018;22(4):867–77.

9. Moghadam BY, Connelly KT, Posner JD. Two orders of magnitude improvement in detection limit of lateral flow assays using isotachophoresis. Anal Chem. 2015;87(2):1009–17.

10. Kim J, Vu B, Kourentzi K, Willson RC, Conrad JC. Increasing Binding Efficiency via Reporter Shape and Flux in a Viral Nanoparticle Lateral-Flow Assay. ACS Appl Mater Interfaces. 2017;9(8):6878–84.

11. He X, Liu Z, Yang Y, Li L, Wang L, Li A, et al. Sensitivity Enhancement of Nucleic Acid Lateral Flow Assays through a Physical-Chemical Coupling Method: Dissoluble Saline Barriers. ACS Sensors. 2019;4(6):1691–700.

12. Bahadır EB, Sezgintürk MK. Lateral flow assays: Principles, designs and labels. TrAC - Trends Anal Chem. 2016;82:286–306.

13. Hu LM, Luo K, Xia J, Xu GM, Wu CH, Han JJ, et al. Advantages of time-resolved fluorescent nanobeads compared with fluorescent submicrospheres, quantum dots, and colloidal gold as label in lateral flow assays for detection of ractopamine. Biosens Bioelectron. 2017;91(October 2016):95–103.

14. Linares EM, Kubota LT, Michaelis J, Thalhammer S. Enhancement of the detection limit for lateral flow immunoassays: Evaluation and comparison of bioconjugates. J Immunol Methods. 2012;375(1–2):264–70.

15. Posthuma-Trumpie GA, Korf J, Van Amerongen A. Lateral flow (immuno)assay: Its strengths, weaknesses, opportunities and threats. A literature survey. Anal Bioanal Chem. 2009;393(2):569–82.

16. Castro C, Rosillo C, Tsutsui H. Characterizing effects of humidity and channel size on imbibition in paper-based microfluidic channels. Microfluid Nanofluidics. 2017;21(2):1–14.

17. Metkar SS, Mahajan SK, Sainis JK. Modified procedure for nonspecific protein staining on nitrocellulose paper using Coomassie brilliant blue R-250. Vol. 227, Analytical Biochemistry. 1995. p. 389–91.

18. Rath D, Sathishkumar N, Toley BJ. Experimental Measurement of Parameters Governing Flow Rates and Partial Saturation in Paper-Based Microfluidic Devices. Langmuir. 2018;34(30):8758–66.

19. Holstein CA, Chevalier A, Bennett S, Anderson CE, Keniston K, Olsen C, et al. Immobilizing affinity proteins to nitrocellulose: A toolbox for paper-based assay developers. Anal Bioanal Chem. 2016;408(5):1335–46.